Prepared for submission to JCAP

# The Maximum Circular Velocity Dependence of Halo Clustering

## Contents



## 1 Introduction

XXX

## 2 The Simulation

We use cosmological N-body simulations called the Bolshoi simulation and the MultiDark simulation, described in XXX and XXX respectively, to investigate the maximum circular velocity dependence of halo clustering. The Bolshoi simulation uses $2048^3$ particles with a volume of $(250h^{\ \ 1}\mathrm{Mpc})^3$, while the MultiDark simulation uses the same number of particles as the Bolshoi simulation but with a volume of $(1h^{\ \ 1}\mathrm{Gpc})^3$. Both simulations assumes a at CDM model with density parameters $_m = 0.27$, $= 0.73$, $_b = 0.0469$, and $_8 = 0.82$, $n = 0.95$, $h = 0.70$. (??Do I need to put a name for each constant?)The details of the simulations are described in XXX. For halo identi cation, we use the ROCKSTAR halo nder (XXX) where the halo masses and maximum circular velocities are computed from bound particles.

??Should I explain more about what bound particles mean (though my understanding is vague...) and am not so sure what other ways to de ne masses and circular velocity and also how the de nitions can make things di erent...

??What other information do I need to put here?

## 3 The Maximum Circular Velocity Dependence of Halo Clustering

In this section, we investigate the maximum circular velocity dependence of halo clustering on both large and small scales. In order to do that, we compute correlation functions and measure halo biases for halo samples having di erent maximum circular velocities. We rst describe how we select halos for each sample and then show how those samples have di erent clustering properties.

As shown in Fig. 1, the maximum circular velocity and halo mass has tight correlation, and yet the scatter between the maximum circular velocity and halo mass becomes larger with decreasing halo masses. In fact, we can compute an expected maximum circular velocity from halo mass

$$V_{\mathrm{max}} = 0.465 M_{\mathrm{vir}}^{1/3} \sqrt{G(\frac{4}{3} \quad _{h} \ _{\mathrm{crit}} \ _{m})^{1/3} \frac{c}{\ln(1+c) \quad c/(1+c)}}; \tag{3.1}$$

where $V_{\mathrm{max}}$ is the maximum circular velocity and $M_{\mathrm{vir}}$ is the halo mass, $_h$ is the overdensity limit which de nes the virial radius, and $c$ is the concentration parameter. Eq. 3.1 comes from an NFW pro le (citation). To obtain Eq. 3.1, we use the concentration of

$$\log_{10} c = \quad 0.097 \log_{10} \mathrm{M}_{\mathrm{vir}} + 2.148. \tag{3.2}$$

(??Ask Frank how he obtain this concentration value and why this is a reasonable value) In Fig. 1, this $V_{\mathrm{max}} \quad M_{\mathrm{vir}}$ relation with the above concentration (shown as a red solid line) intersects the peak of the distribution, which means that many of the halos follow this relation.

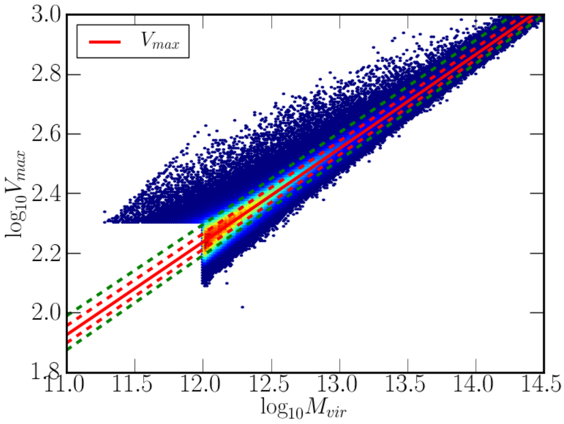


**Figure 1**. Distribution of halo mass and the maximum circular velocity at $z = 0{:}0$ from the MultiDark simulation. The red solid line represents the maximum circular velocity computed for a given halo mass using Eq. 3.1. The red and green dashed lines are 1 and 2 away in the log-normal distribution of concentration at a xed halo mass. ??Add color bar to the plot

In other words, the above equation is a one to one mapping between the virial mass of the halo and its maximum circular velocity. Given this mapping, we can translate clustering measurements as a function of halo mass into predicted clustering measurements as a function of maximum circular velocity. Our goal below is to determine whether this conversion describes the measured clustering or if there is a residual dependence on the maximum circular velocity. In order to explore this, we rst split the sample into a sequence of virial mass bins, chosen such that there are the same numbers of halos in each bin. This process is reminiscent of an abundance-matching procedure (cite XXX). We then further split each bin into two subsamples with their observed $V_{max;obs}$ greater than (denoted by \upper") or less than (denoted as \lower") $V_{max}(M_{vir})$. This selection ensures that both the upper and lower subsamples have the same mean halo mass. Therefore, in the absence of an additional $V_{max}$ dependence (??isn't this $M_{vir}$ dependence?) on clustering, these samples should have the same clustering properties. Note that this would not be true if we had simply split the sample along $V_{max}$, since the two resulting subsamples would have di erent mean halo masses.

In order to measure halo biases, we compute halo-matter cross correlation functions for each subsample and measure a linear bias

$$b_{lin} = < \ _{hm}(r) = \ _{mm}(r) >; \tag{3.3}$$

where $_{hm}$ and $_{mm}$ are halo-matter and matter-matter correlation functions and we take the average of the ratio on $r$ from $10h^{\ 1}$Mpc to $20h^{\ 1}$Mpc where $r$ is the distance between two objects counted on correlation functions (??may change to jackknife samplings). Here, instead of using full DM particles, we subsample 1000000 particles to compute matter auto correlation functions. The reason we use cross correlation functions is to reduce the shot noise e ect on the error.

In Fig. 2, we show how linear biases depend on the maximum circular velocity as a function of halo mass. We compute linear biases for each mass bin classifying into \upper" and \lower" maximum circular velocity halos. The halos which have di erent maximum circular velocity clearly cluster di erently. Furthermore, the relative bias of \upper" versus \lower" subsamples increases with decreasing halo mass to almost 40% on low mass end.

In Fig. 3, we investigate the maximum circular velocity dependence of halo bias on small scales. On small scales, a halo bias is scale-dependent. The question here is whether halos with di erent maximum circular velocity have di erent scale-dependence on their biases. In order to nd that, we take the ratio of halo-matter cross correlation functions between \upper" and \lower" subsamples and normalize it by their linear biases. Fig. 3 clearly shows that the scale-dependence depends on the maximum circular velocity and its Vmax-dependence is mass-dependent. As halo mass decreases, the

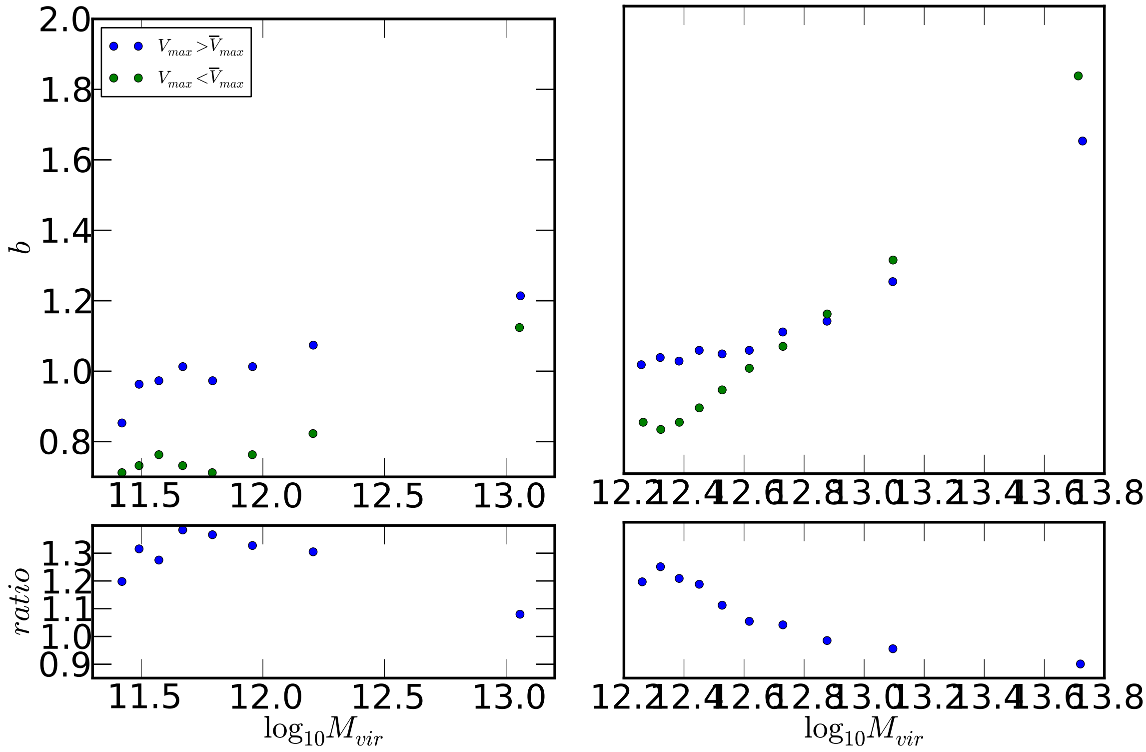


Figure 2. Upper panel: Linear bias at $z$ = 0:0 as a function of halo mass from the Bolshoi simulation (left) and the MultiDark simulation (right). The blue solid line represents a linear bias for halos whose maximum circular velocities are greater than $V_{\rm max}(M_{\rm vir})$ from Eq. 3.1 (labeled as \upper"), while the green solid line corresponds to halos whose maximum circular velocities are smaller than $V_{\rm max}(M_{\rm vir})$ (labeled as \lower"). Lower panel: Ratio of linear biases between \upper" and \lower" maximum circular velocity halos at $z$ = 0:0 from the Bolshoi simulation (left) and the MultiDark simulation (right). As halo masses decrease, the di erence on halo bias between \upper" and \lower" subsamples becomes larger.

relative scale-dependence between \upper" and \lower" subsamples increases, especially halos with large maximum circular velocities heavily clustered around $1h^{\ 1}$Mpc.

*need some explanations for the decrease of the relative bias on the lowest mass end? is it real or arti cial?

*use M*

*use jackknife sampling to put error bars

*where this trend comes from?...assembly bias: concentration?->z_form

*Why is upper subsample clustered around 1Mpc/h? Are there any physical reasons?

*Do we get the same scale-dependence by eliminating ejected halos?

## 4 Discussion

**Figure 3.** Ratio of halo-matter cross correlation functions for \upper" and \lower" subsamples on small scales normalized by their linear biases (normalized!). The plots are from the Bolshoi simulation (left) and the MultiDark simulation (right) at z = 0:0. Each line corresponds to di erent halo mass bins labeled in the plots. Those plots show that \upper" and \lower" subsamples have dierent scale-dependence on small scales and the relative scale-dependence between those subsamples increases smoothly with decreasing halo mass. (?? normalize by their linear biases)

**Figure 4.** ejected halos